An analysis of tropospheric properties of the Mileura site

R.J.Sault
18 October 2005

Introduction

The SKA site submission process requests an analysis of the tropospheric properties of the candidate sites as they relate to the SKA. The request should be viewed in the context of a radio telescope operating at up to 25 GHz. In particular the RFP requests information on

- ? Local tropospheric transparency and "microscopic tropospheric stability"
- ? Diurnal and annual variation of the precipitable water vapour (PWV) content towards the zenith, including statistical insight into its value.

As a form of guidance, a memo has been produced by Erasmus (2005), which gives some insight into analysis that could be used in the site submission process.

The RFP does not suggest measures of "microscopic tropospheric stability". This memo assumes that atmospheric seeing at radio wavelengths is the appropriate information needed to address this.

There are no direct measurements of the relevant quantities at Mileura. To address some of the tropospheric issues in the site submission process, this memo proceeds as follows:

- ? An estimate if made of the expected sky brightness temperature and PWV at the Mileura site, using radiosonde data from Meekatharra.
- ? As a validation of the technique, a similar estimate is made using radiosondes from Moree township. This is compared with actual measurements at the Australia Telescope Compact Array (ATCA) site 100 km south of Moree.
- ? It is argued that Mileura is likely to have broadly similar, if not better, atmospheric seeing characteristics than the ATCA. An analysis of atmospheric seeing at the ATCA site is given as a surrogate of Mileura data.

Transparency and PWV of the Mileura site

The methodology for estimating the transparency and precipitable water vapour at the Mileura site is similar to that used by Erasmus (2005) in analysing radiosondes. Meteorological data is not available for Mileura. Instead data were used for Meekatharra. Meektharra is 100 km further inland (east) than Mileura on the same large plain system of inland Western Australia. Although there will be some differences between the two locations, it is felt that Meekatharra is representative of the conditions at Mileura.

Radiosonde data was obtained for Meekatharra township. Numerical integration along the path of the each radiosonde was used to determine both the PWV and the expected sky brightness temperature at the zenith. Radiosondes were typically available twice per day, with measurements normally at 11:00 and 23:00 UT. A total of 4776 radiosondes were used in the analysis. The measurements consisted of a near complete set from January 1998 to September 2005, plus a small amount of data from 1994. To determine the sky brightness temperature, a numerical integration of the relevant radiative transfer equations (eg Janssen 1992) was performed, using appropriate models of the microwave properties of the tropospheric gases (Liebe 1985). Note:

- The elevation of Meekatharra is 518 m, whereas that of Mileura site is 455 m. The radiosonde measurements were extrapolated to make them representative of a site at 455 m.
- The sky brightness temperatures correspond to zenith ones and include the contribution of the cosmic microwave background.
- The estimates do not include the affects of clouds: clouds are ignored. The presence of water droplets will increase the atmospheric opacity and sky brightness. Note that, on average, 188.2 days/year are classified as "clear" at Meekatharra, whereas 55.8 days are classified as "cloudy".

Figures 1, 2 and 3 give the estimated PWV and sky brightness at 10 and 25 GHz for Mileura as a function of month. The median, 5, 25, 75 and 95 percentile levels are given. Figures 4, 5 and 6 give cumulative histograms of these measures.

Because typically two radiosondes are launched per day at Meekatharra, some insight is possible into the diurnal variation in PWV. Following Erasmus (2005), Figure 7 gives a cumulative distribution function of the difference between a night-time radiosonde PWV estimate and the preceding daytime estimate. In total there were 1918 radiosonde pairs that could be used in this estimate (940 radiosondes had no partner within 14 hours). Figure 7 shows no systematic variation in PWV between night and day, with the estimates suggesting that the variations are 2 mm and less in 50% of pairs. The median variation is near 0 mm. These results are very similar to the results of Erasmus (2005) for Springbok.

Validation: Data from Moree and the ATCA

To help validate the analysis for Mileura, a similar analysis was performed for the town of Moree. Because Moree is felt to be meteorologically very similar to the ATCA, the estimates from radiosonde data can be compared with actual measurements from the ATCA. Note that the ATCA is 100 km south of Moree, and that both are on the western plains of New South Wales. Although plains separate the ATCA and Moree, there is a mountain range (the Nandewar Ranges) 50-60 km to the east/south-east of the ATCA/Moree. The ATCA and Moree are at very similar elevations (210 and 214m respectively).

Radiosonde data available for Moree was analysed in an identical fashion to the Meekatharra data. In total 8612 radiosondes were available for analysis, spanning 1984 to 2005, with a mix of daytime and night-time measurements. Figures 8, 9 and 10 give the PWV and sky brightness estimates with month for Moree. To simplify comparison with Mileura, the information from Figures 1, 2 and 3 are replicated on Figures 8, 9 and 10. It is apparent that the Mileura site is estimated to be better than Moree/ATCA.

To validate the radiosonde technique, direct comparisons with some ATCA data are available. Since July 2005 the ATCA has monitored a radiometer which provides a regular estimate of the zenith sky brightness temperature at 18 GHz. Figure 11 shows cumulative histograms of sky brightness measurements at the ATCA at 18 GHz versus values estimated from Moree radiosonde data for 15 July to 26 September 2005 (77 radiosondes). Overall the general agreement of the two curves is good. Note, however, the following discrepancies:

- There is a difference of about 1 Kelvin between the curves, which is believed to be a real systematic error in the radiosonde approach or radiometer calibration.
- There is an excess amount of sky brightness values larger than 15 K for the ATCA measurements. This difference reflects that the radiosonde modelling does not include

the effect of clouds. More problematically it also reflects that during rain periods the goretex cover sheltering the radiometer becomes wet, and contributes significantly to system temperature. An additional complication is that the sky brightness temperature measurement is available only during observing at the ATCA's highest two frequency bands. There is a bias against using these bands during poor weather.

Overall the measurement statistics and modelling in poorer weather condition is quite uncertain. It is likely that there are significant errors in the sky brightness characterisation in the poorest decile.

Tropospheric stability

The RFP requests that an analysis be made of "microscopic stability" of the troposphere. In radio interferometry, the main instability of concern is atmospheric seeing – the fluctuation in differential excess path through the troposphere as seen by two antennas. This is caused by turbulence in the amount of water vapour along the line of sight. The absolute water vapour content is usually not considered a good measure of the likely seeing. This is because the amount of "turbulent" water vapour is usually quite small (e.g. for points 1km apart, the turbulence seen corresponds to of order 1% of the total water vapour). The amount of turbulence is generally considered to be more important than the total amount of water vapour. Kolmogorov turbulence theory is the methodology commonly used to characterise atmospheric seeing.

No direct measurements of atmospheric seeing are available for the Mileura site. Instead this memo argues that the atmospheric seeing is expected to be broadly similar, if not somewhat better, than the ATCA. An analysis of the atmospheric seeing at the ATCA is then presented as a surrogate for Mileura.

Topography is a significant driver of instability in the atmosphere. As an example, see Lay (1997) for a discussion on the influence of topography on atmospheric seeing at the Owens Valley interferometer. The ATCA is situated in an inland plain where the topography is quite simple. In the upwind direction, it is a considerable distance to mountains and topographic complexity. An analysis of data from the ATCA shows that the turbulence layer is in the ~100 m of the atmosphere closest to the ground. In this case, normal turbulence is a result of convection and the interaction of winds with the ground. In addition to this normal situation, there is turbulence associated with the passage of fronts and storm systems.

Like the ATCA, Mileura is on an inland plain with simple topography and no nearby ranges. It would be expected that, like the ATCA, the turbulence layer would be close to the ground. In terms of ground wind speed, Mileura is marginally windier than the ATCA site. These similarities taken with Mileura's drier nature suggests that overall Mileura seeing should be comparable or better than the ATCA conditions. However the following should also be noted:

- Mileura experiences fewer storms and fronts than the ATCA. Storms and fronts are associated with the worst turbulence at the ATCA. It is likely the poor end of the seeing distribution would not be as poor at Mileura.
- Mileura is, on average, about 3°C warmer than the ATCA site. This suggests convective turbulence, particularly during summer days, may be more excessive. It may be that Mileura has poorer conditions during summer days than does the ATCA. It is unclear whether this effect would be countered by Mileura's drier conditions.
- At the ATCA, a deep inversion layer can form on some cold winter nights. These present the best high frequency observing conditions at the ATCA. Wind

measurements suggest these conditions are less common at Mileura. Consequently the very best conditions at Mileura may be poorer than at the ATCA.

The ATCA has an atmospheric seeing monitor. The following analysis uses measurements from 260 days spanning from 11 September 2004 to 18 October 2005. Unfortunately no data is available for February and March, and there is only limited data available for January. The ATCA seeing monitor is a simple interferometer that observes a geostationary satellite at 30 GHz. The baseline length is 230 m, and the satellite is at an elevation of 60°.

In the standard Kolmogorov model, the atmospheric seeing is characterized by

$$f(b) = f_o (b/b_o)^{ß}$$

where f is the rms excess path between two antennas with baseline b apart. Theory suggests that the power law exponent, ß, depends on whether the turbulent layer of the troposphere is "thin" ("2D turbulence", when the layer width is less than the baseline length) or "thick" ("3D turbulence", where the layer width greater than the baseline length). Power law exponents of 0.83 and 0.33 are expected for 3D and 2D turbulence respectively)

The ATCA generates measurements of f , ß, and v_s - a measure of the speed of the phase screen (the so-called "wind velocity aloft"). A technique similar to the approach of Holdaway et al (1995) is used to derive the measurements from the raw phase measurements. To simplify comparison with other measurements, f is expressed in microns of excess path, and adjusted to correspond to a zenith value for antennas separated by b = 1 km. Figures 12, 13 and 14 give cumulative distributions of f , ß, and v_s. The median value of f is 816 microns. However the value of f has significant annual and diurnal variations. Figure 15 gives a plot of the variation of the median value of f with time of day. The different lines correspond to the different months. Figure 16 shows the monthly medians, quartiles, 5 and 95 percentiles. Given that these plots are derived from a single year's data, some care is needed in their interpretation. For example the figures suggest that May is the month with the best seeing conditions. However May in 2005 was unusually dry, and June/July/August 2005 experienced a once in 10 year wet spell (Australian Bureau of Meteorology, 2005).

In interpreting the figures, it is clear that summer days are the worst times in terms of atmospheric seeing: summer days are about 8 times worse than winter nights (Figure 15). Surprisingly, from the perspective of seeing, summer nights are better than winter days.

Note the median Kolmogorov exponent is 0.56 (Figure 13). This value indicates conditions are in a transition domain between 3D and 2D turbulence. This implies that the phase screen depth is comparable to the baseline length of 230m. An additional interesting observation is that the cumulative distribution function of the phase screen speed (Figure 14) resembles the wind statistics in the lowest ~100 m of the atmosphere (as inferred from Moree radiosonde data). It is significantly different from the wind speed at the ground, as well as wind speeds at an altitude of more that ~100m above the ground.

The above two observations suggest that the turbulent layer is comparatively thin, and close to the ground. This conclusion is consistent with an excess amount of water vapour seen in the Moree radiosonde measurements: whereas models of water vapour content usually suggest that water vapour concentration falls off exponentially with a scale height of ~2 km, the Moree radiosonde data show an extra component close to the ground.

Conclusion

Using estimates derived from Meekatharra radiosonde measurements, and using atmospheric seeing measurements at the ATCA as a surrogate, information has been gathered on the likely tropospheric conditions at the Mileura SKA site. The Mileura site is likely better than the ATCA site for observations near 25 GHz, both in terms of atmospheric opacity and seeing. It is possible that Mileura is poorer in terms of atmospheric seeing during summer daytime, and possibly it will not experience the very best observing conditions seen at the ATCA. However it will suffer from less degradation of performance resulting from storms and fronts.

Reference

Erasmus, D.A., 2005, "Precipitable water vapour at SKA Telescope candidate sites: Derivation from rawinsonde data and a discussion of alternative measurement methods", SKA Memo

Janssen, M.A. ed., 1992, *Atmospheric remote sensing by microwave radiometry*, Wiley

Lay, O.P., 1997, "The temporal power spectrum of atmospheric fluctuations due to water vapour", A&AS, 122, 535

Liebe, H.J., 1985, "An updated model for millimeter wave propagation in moist air", *Radio Science*, 20, 1069

Holdaway, M.A., Radford, S.J.E., Owen, F.N., Foster, S.M., 1995, "Data processing for site test interferometers", MMA Memo 129

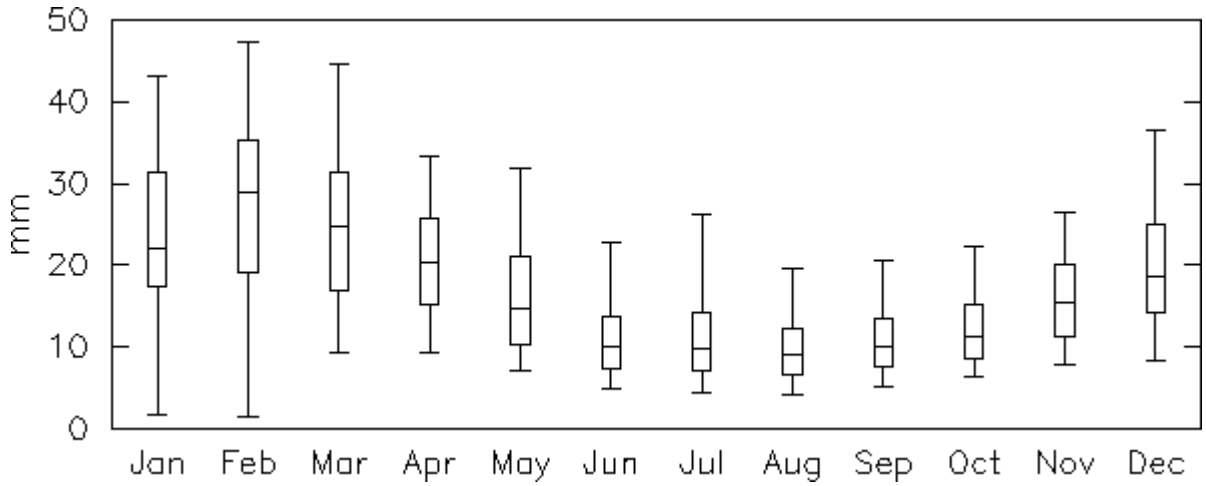

Figure 1: Monthly median, quartiles (box limits) and 5 and 95 percentiles (line limits) of the estimated Mileura precipitable water vapour.

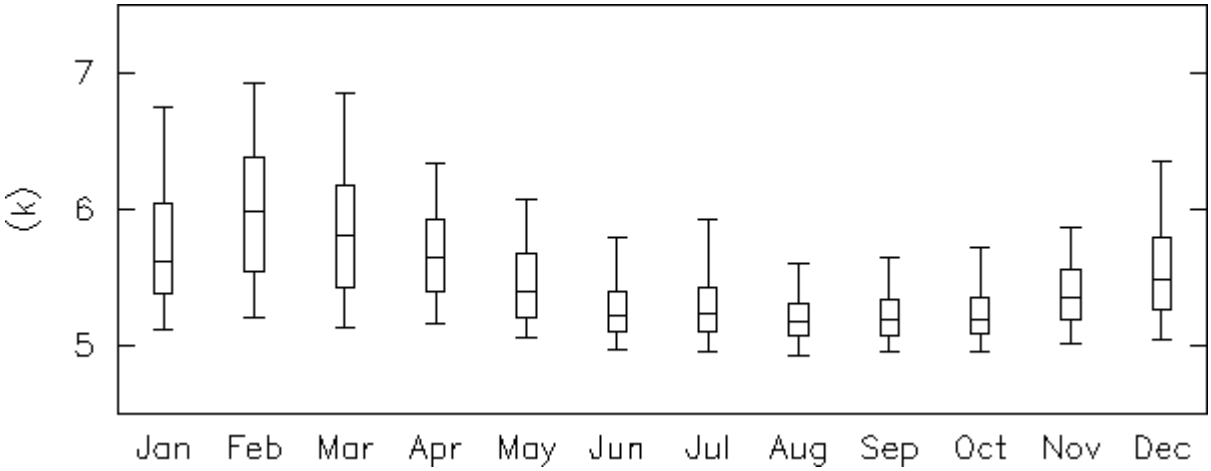

Figure 2: Monthly median, quartiles (box limits) and 5 and 95 percentiles (line limits) of the estimated Mileura 10 GHz zenith sky brightness temperature.

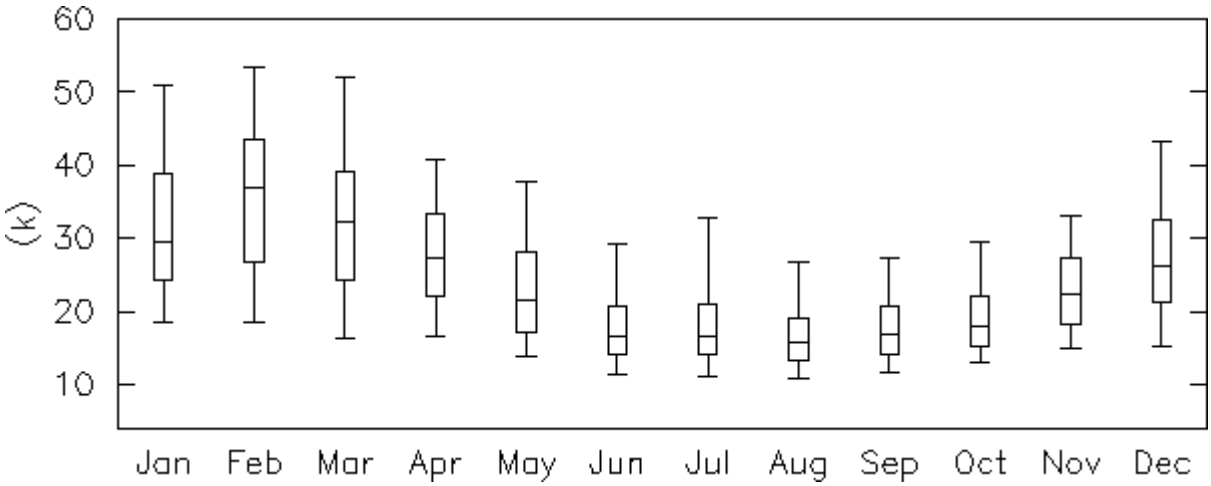

Figure 3: Monthly median, quartiles (box limits) and 5 and 95 percentiles (line limits) of the estimated Mileura 25 GHz zenith sky brightness temperature.

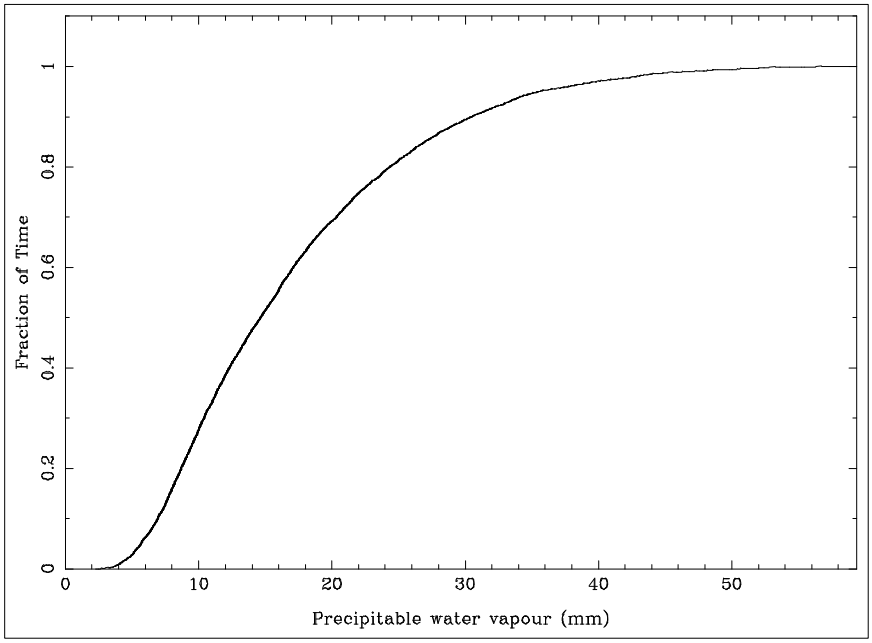

Figure 4: Cumulative distribution function of the estimated precipitable water vapour at the Mileura site.

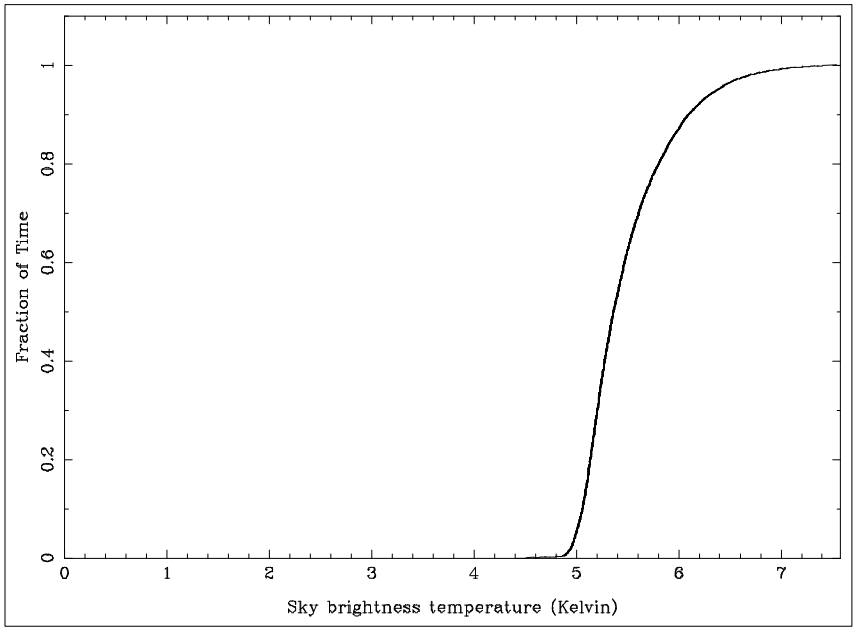

Figure 5: Cumulative distribution function of the estimated zenith sky brightness temperature at 10 GHz at the Mileura site.

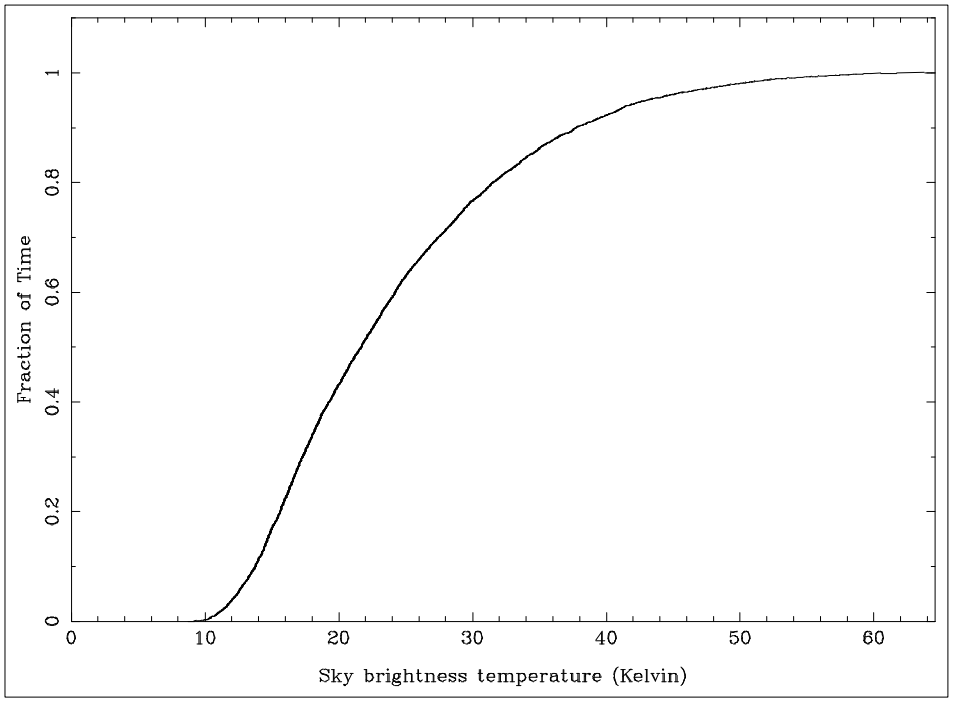

Figure 6: Cumulative distribution function of the estimated zenith sky brightness temperature at 25 GHz at the Mileura site.

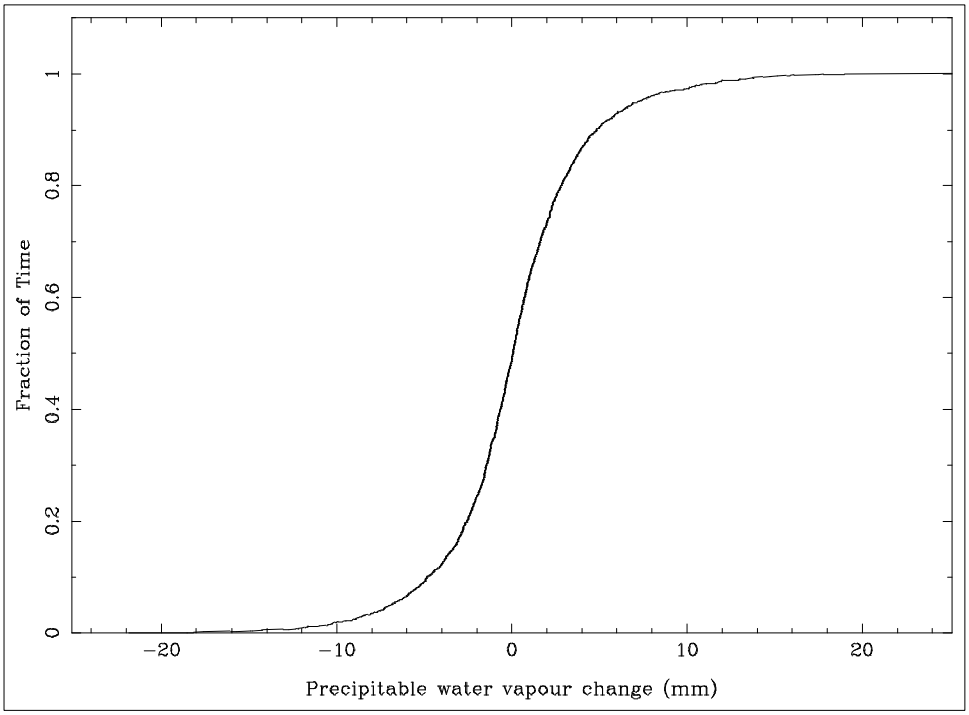

Figure 7: Cumulative distribution function of the change between a night and the preceding day's estimate of the precipitable water vapour at the Mileura site.

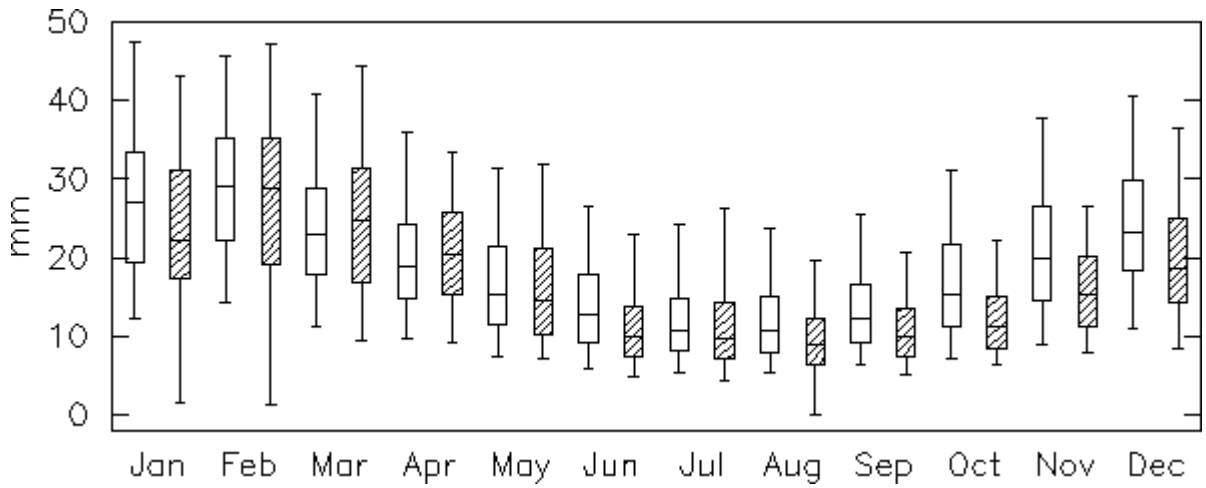

Figure 8: Monthly median, quartiles (box limits) and 5 and 95 percentiles (line limits) of the estimated Moree (unshaded) and Mileura (shaded) precipitable water vapour.

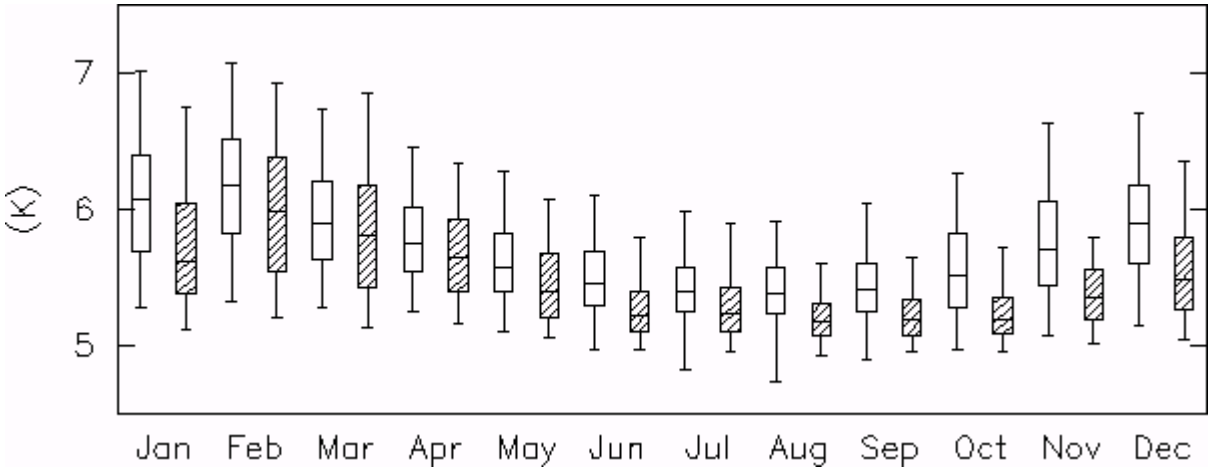

Figure 9: Monthly median, quartiles (box limits) and 5 and 95 percentiles (line limits) of the estimated Moree (unshaded)and Mileura (shaded) 10 GHz zenith sky brightness temperature.

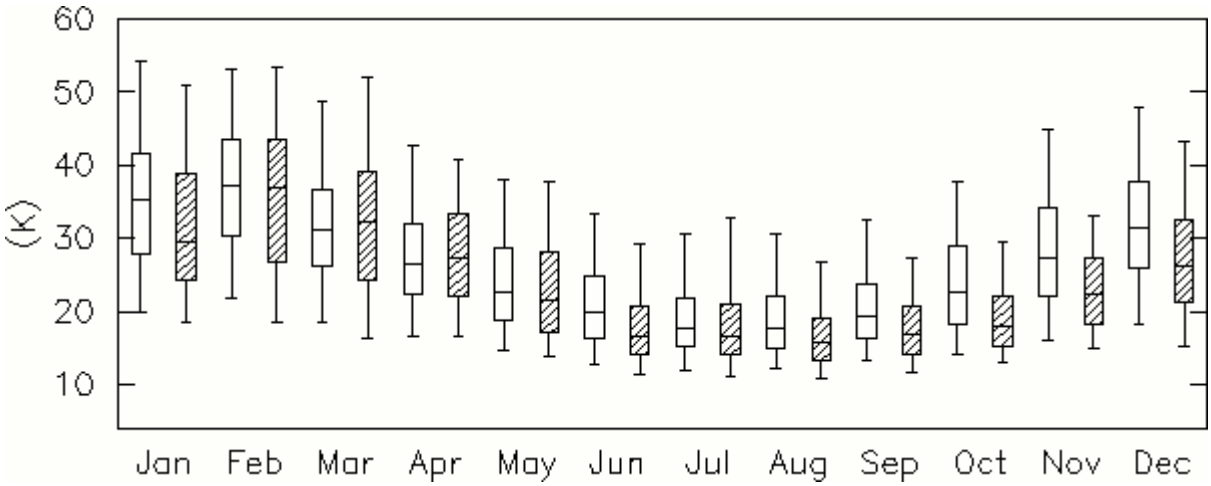

Figure 10: Monthly median, quartiles (box limits) and 5 and 95 percentiles (line limits) of the estimated Moree (unshaded) and Mileura (shaded) 25 GHz zenith sky brightness temperature.

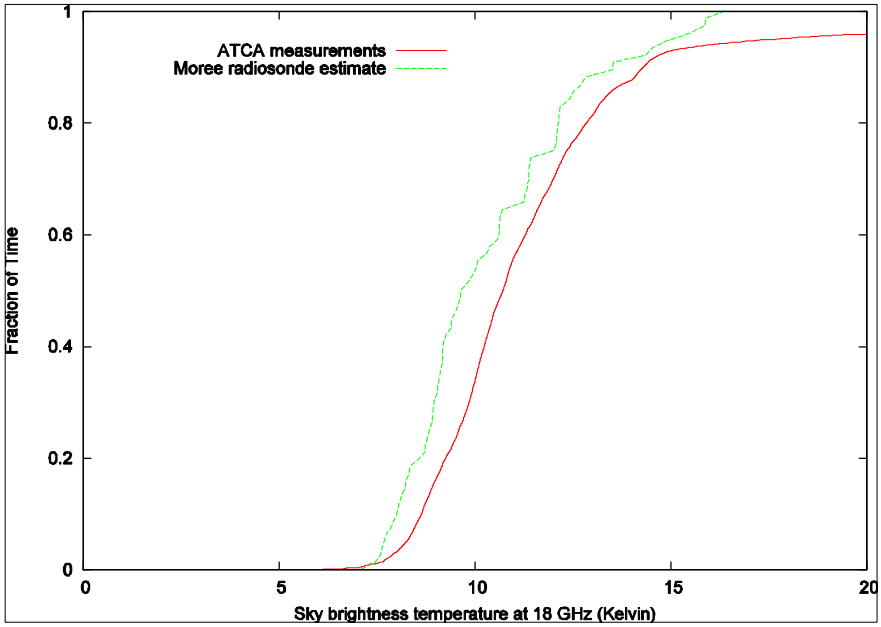

Figure 11: Comparison of cumulative distribution functions of zenith sky brightness temperatures at 18 GHz. The two curves correspond to measurements by an ATCA radiometer and estimates from Moree radiosondes.

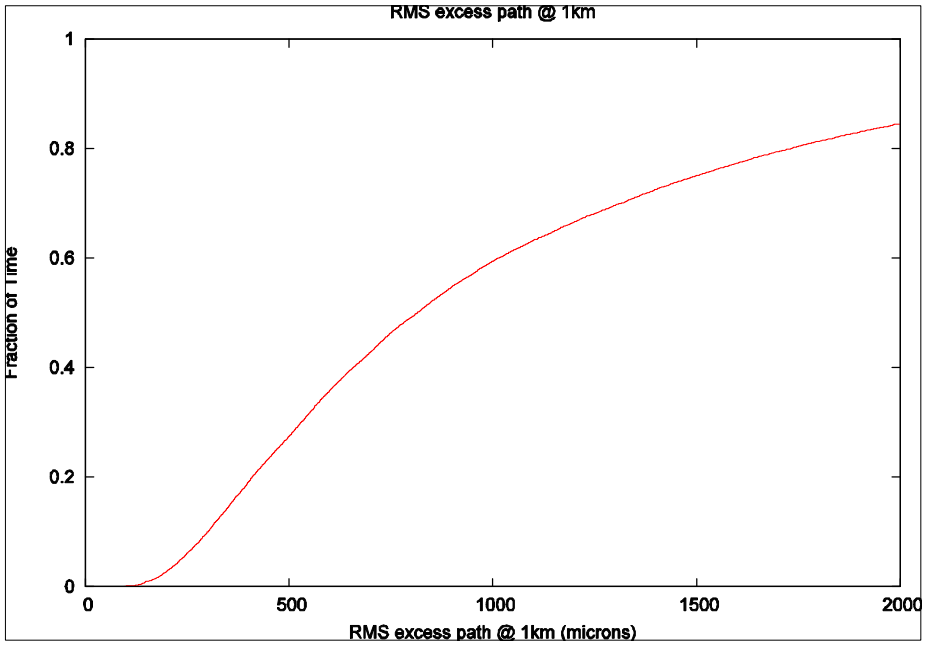

Figure 12: Cumulative distribution function of the rms excess path between two antennas 1km apart, as measured by the ATCA seeing monitor.

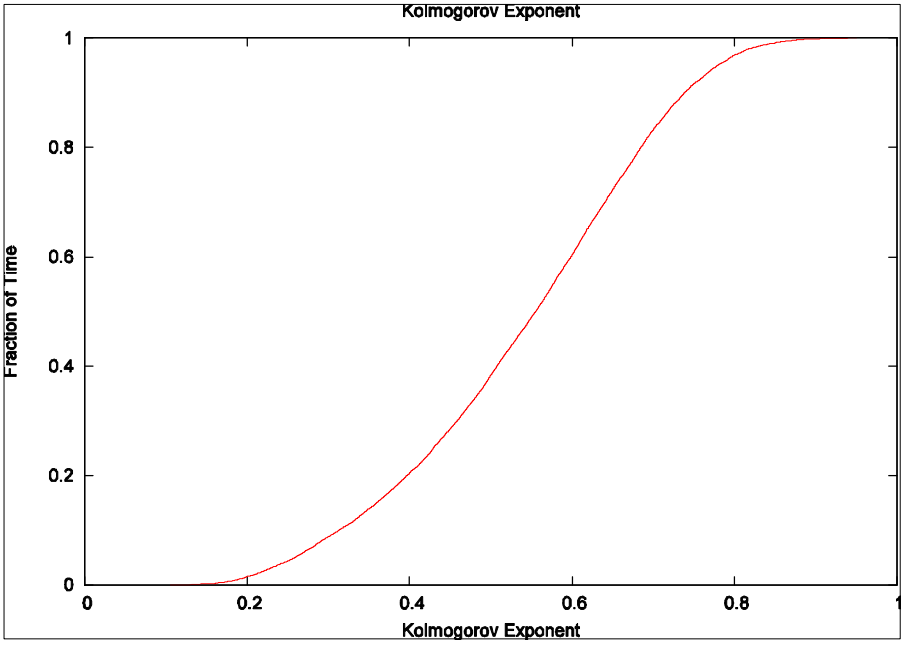

Figure 13: Cumulative distribution function of the phase structure function Kolmogorov exponent, as deduced from the ATCA seeing monitor data.

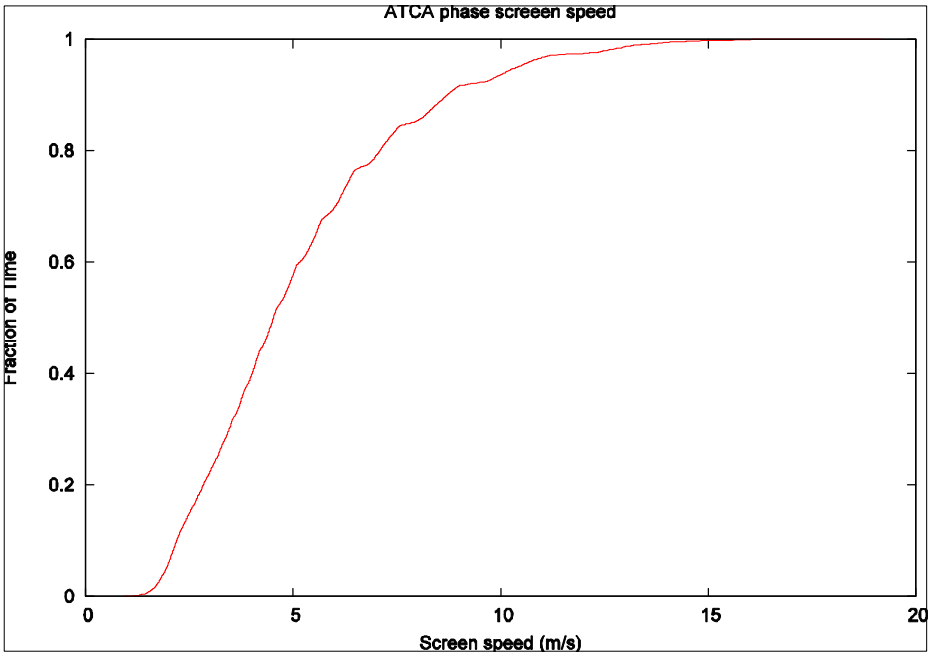

Figure 14: Cumulative distribution function of the deduced phase screen speed ("velocity aloft") as deduced from the ATCA seeing monitor data.

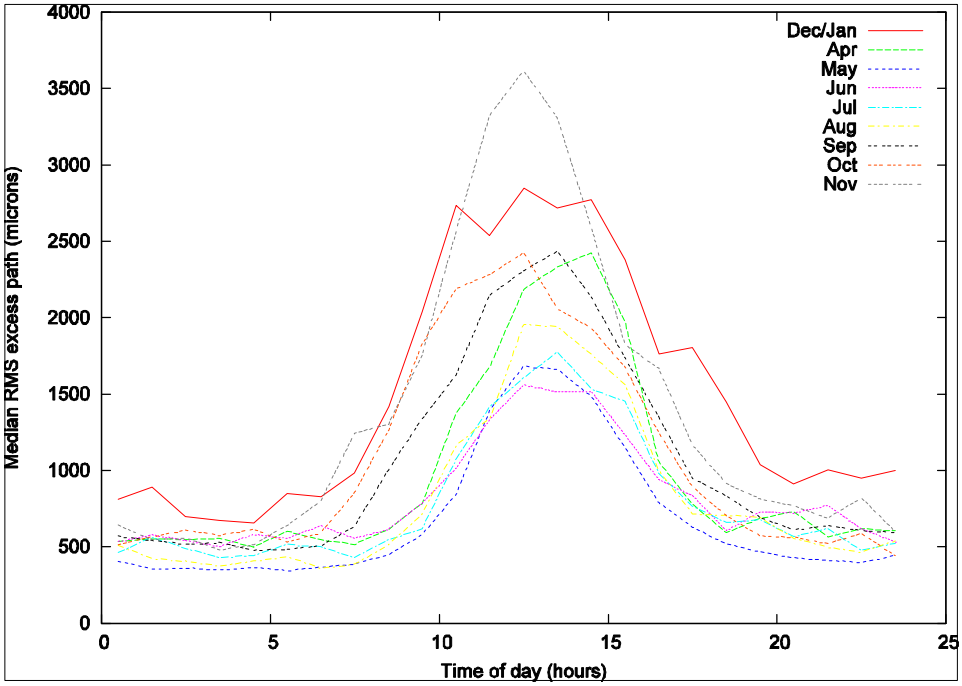

Figure 15: Median rms excess path, for 1 km baselines at the ATCA, as a function of time-of-day, and month.

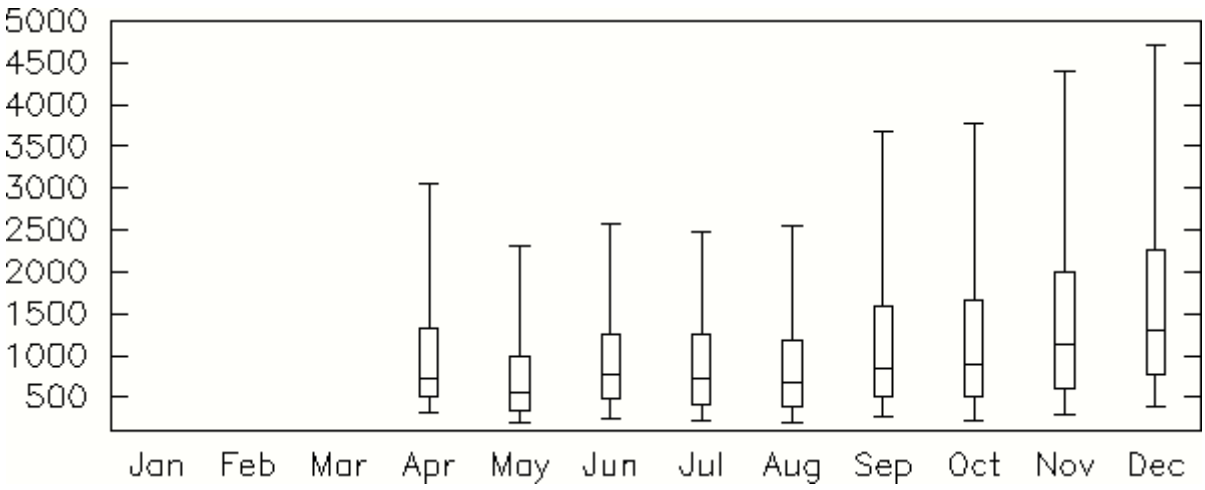

Figure 16: Monthly median, quartiles (box limits), 5 and 95 percentiles (line limits) of the rms excess path, for a 1 km baseline, at the ATCA. No data is available for February and March. Limited data is available for January. January data are included within the December statistics.